Bulgarian Chemical Communications, Volume 53, Issue 2 (pp. 163 - 173) 2021 DOI: 10.34049/bcc.53.2.5301

Modeling and simulating of heat transfer for three-layer skin using an external thermal pulse

R. K. Yaghoobi[1], Masoud Khajenoori[2*], Maryam Khajenoori[2]

[1]*Association of Freelance Researchers, Ferdows, Iran*
[2]*Faculty of Chemical, Gas and Petroleum Engineering, Semnan University, Semnan, Iran*

Received: June 29, 2020; Revised: December 23, 2020

The skin heat transfer models have attracted many researchers in recent years for improving the hyperthermia techniques and for evaluating burn injuries. Nevertheless, many of these researchers, which used the one-layer skin heat transfer model, could not provide useful information about the heat transfer in the laminar structure of skin tissue. Some researchers, which used the multi-layer skin heat transfer model, have questionable results in some cases. Therefore, in this study, we first developed a one-dimensional heat transfer model for a three-layer skin. Then, we investigated the effect of blood perfusion in this heat transfer model under the conditions of thermal equilibrium and the conditions of applying the external thermal pulse to the skin surface. For this work, we provided a direct solution for the conditions of thermal equilibrium and an approximate solution using a finite-difference method (FDM) for the conditions of applying an external thermal pulse. Finally, we evaluated the amount of thermal expansion and damage resulted from different thermal pulses and blood perfusion rates. Generally, the results of this study revealed that the blood perfusion rate has a large influence on the temperature distribution, thermal expansion and thermal damage, so that it significantly can lessen the burn degree, especially of the dermis and subcutaneous fat layers. Nevertheless, skin surface temperature according to the arterial blood temperature can completely reverse the effects of the blood perfusion rate in the temperature distribution of skin tissue. These results also showed that different structural and thermal properties of skin layers, especially thickness and thermal conductivity along with the blood vessels penetrated in the skin layers, can turn the skin tissue into a special thermal insulator, which well disagrees with any change in temperature in the skin surface.

Keywords: Three-layer skin model, Heat transfer, Pennes model, Thermal damage

INTRODUCTION

Skin is one of the most important thermoregulation organs in the human body that continuously regulates the temperature of internal tissues by using different modes of heat transfer such as conduction, convection, radiation and perspiration [1]. Hence, understanding the heat transfer process in the skin is a major challenge in the thermodynamic studies to improve local hyperthermia techniques [2-7] and also evaluate the burn injuries [8].

The main objective of local hyperthermia techniques is also to raise the temperature of the diseased tissue to a therapeutic value above the core temperature, and then thermally destroy it [9-11]. Accordingly, the therapeutic value is a very important factor in this therapy. However, there is no consensus as to what is the safest or most effective target temperature for hyperthermia. For example, some researchers defined this value for the local hyperthermia between 39.5 and 40.5°C [12] and some others defined it between 41.8 and 42°C (Europe, USA) to near 44°C (Japan, Russia) [13]. Furthermore, current studies have confirmed that the heat transfer within the skin is a heat conduction process coupled with physiological processes such as blood perfusion, gland activity, tissue metabolism and sometimes heat losses of the hair [1, 14, 15], so that these physiological processes can create different self-regulation activities by changing the characteristics of each of the skin layers. Therefore, finding an optimal thermal pattern for local hyperthermia techniques and evaluating burn injuries request comprehensive information for the heat transfer mechanism of skin tissue.

Currently, various histological studies have been done on body tissues, especially skin tissues. Nevertheless, although these studies have provided remarkable results about macroscopic parameters such as the core temperature, these studies, due to laboratory and technical limitations, could not usually provide useful information about the temperature distribution of skin layers. Hence, researchers have often focused on mathematical models based on Fourier's heat transfer law for understanding the heat transfer mechanism of skin layers. In this regard, Pennes [16], who proposed a bio-heat transfer equation based on this law, is one of the researchers that have provided a general model for evaluating heat transfer in different body tissues. It is remarkable that this bio-heat transfer equation is currently the basis of many studies in thermal

* To whom all correspondence should be sent:
E-mail: khajenoori1390@gmail.com

diagnostics [17], thermal parameter estimation [18-20] and burn injury evaluation [8, 21, 22] for evaluating different modes such as different boundary conditions and blood perfusion rates. For example, Vyas and Rustgi [23] obtained an analytical solution based on a cylindrically symmetric model (in which the laser beam is traveling only in the z-direction) to study the laser-tissue interaction. Newman [24] investigated the thermal washout in biological tissues by using Green's function method. Zhu and Weinbaum [25] applied the Green's function method to solve a series of steady-status bio-heat transfer problems in which the Pennes' perfusion term was not included. Durkee and Antich [26, 27] addressed the time-dependent Pennes' equation in 1-D multi-region Cartesian and spherical geometry. Lagendijk *et al.* [28] also contributed to understanding some specific heat transfer problems during a tumor hyperthermia process. Kengne [29] investigated the effect of the temperature-dependent thermal conductivity on the nonlinear temperature distribution by using the Taylor expansion method. Deng [30] analyzed the Pennes bio-heat transfer equation for one-layer skin influenced by various heat sources. In [1, 14, 15] Xu *et al.* analytically examined the biothermomechanic behavior of skin tissue under various boundary conditions by using the one-layer Pennes bio-heat transfer equation. They also examined the biothermomechanic behavior in the multi-layer Pennes by the bio-heat transfer equation using the finite-difference method. Lin and Chou [31] proposed a numerical scheme combined with differential transform and finite-difference methods for solving the Pennes bio-heat transfer equation. They examined the one-layer skin heat transfer model in the constant temperature surface. Lai and Chan [32] developed a two-dimensional heat transfer model for a 12-segment human body. They stated that their model was validated for predicting skin and body core temperatures under a wide range of thermal conditions. Strakowska *et al*. also evaluated the Pennes bio-heat transfer equation for a skin tissue, in which each of the three layers had different thermal parameters. These researchers finally reported that there was a rate of significant fitting between the temperature of the skin surface estimated by the Pennes equation and temperature recorded by a thermal camera from the skin surface in a certain time interval [33].

Generally, although these studies provided interesting results in some cases for improving the therapeutic applications, their results were questionable in some cases. For example, some of these researchers [1, 14, 15] reported that an external heat source in addition to the strain caused by thermal expansion generates a mechanical strain, while a thermal loading (external heat source) based on the solid mechanics only generates thermal strain in the solid material. Some other researchers [1, 30], which investigated the influence of blood perfusion rate on the temperature distribution of skin tissue, also considered that increasing the blood perfusion rate generally decreases the temperature distribution of skin tissue, while the temperature of skin tissue in addition to the blood perfusion rate depend on air temperature adjacent to skin surface. On the other hand, the human skin consists of three layers: the epidermis, the dermis and the subcutaneous layer. The two internal layers, especially the subcutaneous layer is primarily made up of fat and connective tissue [34]. It is remarkable that the fat insulates the body against both heat and cold. Therefore, the thermal response of these layers to an external heat source can turn from a conductor to an insulator and conversely [34], because the fat layers act as a thermal inductor against heat. This means that the temperature distribution resulted from an external heat source has special dynamics. Nonetheless, some of these researchers [1, 14, 15], who examined the heat transfer in the three skin layers, did not report such dynamics. Furthermore, it is also amazing that other researchers have reported their outcomes at temperatures above 45°C regardless of the fact that at temperatures above 45°C the skin changes due to the burn. This is another questionable result of these researches.

Therefore, in this study, we provided a one-dimensional bio-heat transfer model based on the Pennes equation that presented interesting results about the dynamics of skin heat transfer and also the thermal expansion and damage caused by an external heat source on the three skin layers. The remainder of this paper is organized as follows: Sections 2 and 3 present the heat transfer equations and boundary conditions of the proposed model for three skin layers. Section 4 provides equilibrium temperature distribution in the three skin layers by solving the equations of the proposed model under the condition of thermal equilibrium of skin tissue. Section 5 shows the total temperature distribution resulted from a thermal pulse applied on the skin surface which obtained from the solution the equations of the proposed model by using the backward finite-difference method (BFDM), which is also known as the backward Euler method. Sections 6 and 7 provide the thermal expansion and damage created by different thermal pulses and blood perfusion rates. Finally, section 8 presents a brief conclusion about the results obtained in this research.

Heat transfer equations of a three-layer skin

As stated, the heat transfer in the skin layers is a heat conduction process coupled with blood perfusion. Hence, this process is also dependent on the size of the blood vessels. In addition, since the thermal equilibration length of blood vessels (L_{eq})

[35, 36] in the skin tissue is significantly shorter than the length of the blood vessel in this tissue, i.e. about 2×10^{-5} to 3×10^{-5} mm [1, 37], the temperature of ejected blood through the vessels is approximately equal to the temperature of the skin tissue. These conditions also confirm that the Pennes bio-heat transfer equation suffices to model the heat transfer in the two internal layers of the skin [1, 38]. It is also suitable to model the heat transfer in the outer layer of the skin.

The Pennes equation is a derivation of Fourier's heat transfer equation and general bio-heat transfer equation [16]. This equation is defined as follows:

$$\rho c \frac{\partial T}{\partial t} = k \frac{\partial^2 T}{\partial z^2} + Q_{met} + Q_b(T) \tag{1}$$

where ρ, c and k are the density, specific heat and thermal conductivity of the skin tissue, respectively. Q_{met} is the metabolic heat generation in the skin tissue and Q_b is the heat generated by vessels and is expressed as follows:

$$Q_b(T) = \omega_b \rho_b c_b (1-\mu)(T_a - T) \tag{2}$$

where ρ_b and c_b refer to blood. ω_b is the blood perfusion rate. T_a and T are the temperature of arterial blood and skin tissue, respectively. μ has been usually considered equal to zero [1, 16, 31]. It also seems that this parameter is a thermal friction coefficient, which Pennes added to its equation and considered that its value can be between 0 and 1.

Proposed model for three skin layers

In this work, we investigated the heat transfer in one-dimension for three layers of the skin (see Fig. 1). This approximation is good when the heat is propagated in the direction perpendicular to the skin surface (e.g. during laser heating). As shown in Fig. 1, we assumed the skin tissue as three cubes with infinite length and width, and finite depth. Therefore, we simplified the Laplace operator in equation (1) for each of the skin layers as equation (3). In other words, we actually used a one-dimensional model as outlined at the beginning of the next subsection.

$$\nabla^2 T = \frac{\partial^2 T}{\partial z^2} \tag{3}$$

Accordingly, by using equations (1) and (3) we rewrote the heat transfer equations for each of the three skin layers as follows:

$$\begin{cases} \rho_e c_e \dfrac{\partial T_e}{\partial t} = k_e \dfrac{\partial^2 T_e}{\partial z^2} + Q_{e,met} \\ \rho_d c_d \dfrac{\partial T_d}{\partial t} = k_d \dfrac{\partial^2 T_d}{\partial z^2} + Q_b(T_d) + Q_{d,met} \\ \rho_f c_f \dfrac{\partial T_f}{\partial t} = k_d \dfrac{\partial^2 T_f}{\partial z^2} + Q_b(T_f) + Q_{f,met} \end{cases} \tag{4}$$

Notations *e*, *d* and *f* represent the epidermis, dermis and subcutaneous fat layers, respectively. As seen in the equation relevant to the epidermis layer, we do not consider the blood perfusion term for this layer, because the blood perfusion of this layer is negligible. We also assumed that the heat wasted through sweat glands and hairs is negligible and the thermal properties of skin layers are homogeneous. In the next section, we provided the boundary conditions for each of the skin layers.

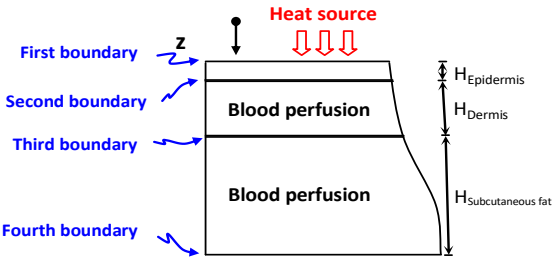

Fig. 1. The corresponding idealized skin model

Boundary conditions of three-layer skin

As shown in Fig. 1, there are four boundaries in the one-dimensional heat transfer model for three-layer skin. The first boundary is related to the temperature of the skin surface that is equivalent to the temperature generated by the external heat source on this surface. The second boundary is located between the epidermis and dermis layers. Similarly, the third boundary is located between the dermis and the subcutaneous fat layer. Second and third boundaries have the same temperature and heat flux profiles. The last boundary is between the subcutaneous fat layer and the internal layer (fat layer). The temperature of this boundary is approximately equal to the core temperature, i.e. ~37°C [39]. Therefore, we defined the boundary conditions of the three skin layers as follows:

$$\begin{cases} C_1: & T_e(0,t) = Q_{ext}(t) \\ C_2: & T_e(H_e,t) = T_d(0,t) \\ C_3: & k_e \dfrac{\partial T_e(H_e,t)}{\partial z} = k_d \dfrac{\partial T_d(0,t)}{\partial z} \\ C_4: & T_d(H_d,t) = T_f(0,t) \\ C_5: & k_d \dfrac{\partial T_d(H_d,t)}{\partial z} = k_f \dfrac{\partial T_f(0,t)}{\partial z} \\ C_6: & T_f(H_f,t) = T_C \end{cases} \quad (5)$$

where T_c is the core temperature. In the next section, we solved the equations of the proposed model under the conditions of thermal equilibrium of skin tissue.

Equilibrium temperature distribution

As we know, the equilibrium temperature distribution in the three skin layers can be obtained through solving equations (4) at time t = 0. Therefore, we can rewrite the heat transfer equations of the three skin layers under the conditions of thermal equilibrium as:

$$\begin{cases} a: & k_e \dfrac{\partial^2 T_e(z_e,0)}{\partial z_e^{\,2}} + Q_{e,met} = 0 \\ b: & k_d \dfrac{\partial^2 T_d(z_d,0)}{\partial z_d^{\,2}} + \omega_b \rho_b c_b (1-\mu)(T_a - T_d(z_d,0)) + Q_{d,met} = 0 \\ c: & k_f \dfrac{\partial^2 T_f(z_f,0)}{\partial z_f^{\,2}} + \omega_b \rho_b c_b (1-\mu)(T_a - T_f(z_f,0)) + Q_{f,met} = 0 \end{cases} \quad (6)$$

Similarly, we rewrote the boundary conditions in t = 0 as equations (7), with the exception that we replaced the first boundary condition (C_1 in equations (5)) with a new boundary condition (C_1 in equations (7)), because this boundary, due to $Q_{ext}(0) = 0$ exchanges the heat of skin surface as the convective. Therefore, this new boundary condition is equivalent to heat flows exchanged between the skin surface and the air. In these equations, T_{air} is the air temperature in adjacent to the skin surface. h_{air} is also the heat convection coefficient between the skin surface and the surrounding air.

$$\begin{cases} C_1: & -k_e \dfrac{\partial T_e(0,0)}{\partial z_e} = h_{co}[T_{air} - T_e(0,0)] \\ C_2: & T_e(H_e,0) = T_d(0,0) \\ C_3: & k_e \dfrac{\partial T_e(H_e,0)}{\partial z_e} = k_d \dfrac{\partial T_d(0,0)}{\partial z_d} \\ C_5: & T_d(H_d,0) = T_f(0,0) \\ C_4: & k_d \dfrac{\partial T_d(H_d,0)}{\partial z_d} = k_f \dfrac{\partial T_f(0,0)}{\partial z_f} \\ C_6: & T_f(H_f,0) = T_C \end{cases} \quad (7)$$

Table 1. Values employed for the parameters of the proposed model

Variant	Value	Unit
Blood density	1060	Kg/m^3
Blood specific heat	3770	J/Kg.°C
Density		
Epidermis	1190	Kg/m^3
Dermis	1116	
Subcutaneous fat	971	
Skin specific heat		
Epidermis	3600	J/Kg°C
Dermis	3300	
Subcutaneous fat	2700	
Thermal conductivity		
Epidermis	0.235	W/m°C
Dermis	0.445	
Subcutaneous fat	0.185	
Thickness		
Epidermis (H_e)	0.1	mm
Dermis (H_d)	1.5	
Subcutaneous fat (H_f)	4.4	
Metabolic heat generation		
Epidermis	368.1	W/m^3
Dermis	368.1	
Subcutaneous fat	368.1	
Thermal expansion coefficient		
Epidermis	1e-4	1/°C
Dermis	1e-4	
Subcutaneous fat	1e-4	
Body core temperature (T_C)	37	°C
Arterial blood temperature (T_a)	37	°C
Air temperature (T_{air})	25	°C

Table 1 provides the values employed for the parameters of the proposed model. According to these values, the characteristic equation obtained from the differential equations (6b) and (6c) have a delta greater than zero ($\Delta>0$). Therefore, the general solution of these differential equations is as follows:

$$\begin{cases} T_e(z_e,0) = \dfrac{-Q_{e,met}}{2k_e} z_e^{\,2} + Az_e + B \\ T_d(z_d,0) = Ce^{x_d z_d} + De^{-x_d z_d} + y_d \\ T_f(z_f,0) = Ee^{x_f z_f} + Fe^{-x_f z_f} + y_f \end{cases} \quad (8)$$

$$\begin{cases} x_d = \sqrt{\dfrac{\omega_b \rho_b c_b (1-\mu)}{k_d}} \\ x_f = \sqrt{\dfrac{\omega_b \rho_b c_b (1-\mu)}{k_f}} \\ y_d = T_a + \dfrac{Q_{d,met}}{\omega_b \rho_b c_b (1-\mu)} \\ y_f = T_a + \dfrac{Q_{f,met}}{\omega_b \rho_b c_b (1-\mu)} \end{cases}$$

The particular solution of these equations by using the boundary conditions provided in equations (7) creates a system of linear equations as follows:

$$M.W = P \quad (9)$$

$$M = \begin{bmatrix} k_e & -h_{co} & 0 & 0 & 0 & 0 \\ H_e & 1 & -1 & -1 & 0 & 0 \\ k_e & 0 & -k_d x_d & k_d x_d & 0 & 0 \\ 0 & 0 & e^{x_d H_d} & e^{-x_d H_d} & -1 & -1 \\ 0 & 0 & k_d x_d e^{x_d H_d} & -k_d x_d e^{-x_d H_d} & -k_f x_f & k_f x_f \\ 0 & 0 & 0 & 0 & e^{x_f H_f} & e^{-x_f H_f} \end{bmatrix}$$

$$W = \begin{bmatrix} A \\ B \\ C \\ D \\ E \\ F \end{bmatrix} \quad , \quad P = \begin{bmatrix} -h_{co} T_{air} \\ y_d + \dfrac{Q_{e,met} H_e^{\,2}}{2k_e} \\ Q_{e,met} H_e \\ y_f - y_d \\ 0 \\ T_C - y_f \end{bmatrix}$$

Solving this system of linear equations by using the Gauss-Jordan elimination method [40] gets the coefficients (A-F) of equations (8). Table 2 summarizes these coefficients for three different blood perfusion rates at air temperature of 25°C and 40°C, which we calculated by the Gauss-Jordan elimination method.

Fig. 2 shows the simulation results of equations (8) by using these coefficients. As shown in Fig. 2, the equilibrium temperature distribution in the three skin layers depends on the blood perfusion rate (ω_b) and the air temperature in the adjacent to the skin surface (T_{air}), so that if the air temperature is lower than the arterial blood temperature, increasing the blood perfusion rate exponentially enhances the temperature of the three skin layers (Fig. 2a) and if the air temperature is higher than the arterial blood temperature, increasing the blood perfusion rate exponentially reduces the temperature of three skin layers (Fig. 2b). Therefore, the blood perfusion rate is one of the effective self-regulatory activities in the skin tissues for returning the skin temperature to the arterial blood temperature. The air temperature also plays an important role in this distribution, because self-regulatory activities (brain and heart activities) in the human body always try to hold 37°C for the core temperature by changing the blood perfusion rate.

Table 2. Coefficients of equations (8) under three different blood perfusions

T_{air}	ω_b	A	B	C	D	E	F
25 °C	0.01	862.38	35.13	-0.14	-1.65	0.02	-1.29
	0.001	710.54	33.35	0.14	-3.82	1.12	-4.27
	0.0001	666.05	32.83	3.35	-8.38	6.68	-11.19
40 °C	0.01	-214.86	37.48	0.03	0.41	-0.01	0.32
	0.001	-175.70	37.94	-0.08	0.90	-0.33	1.02
	0.0001	-164.21	38.07	-1.38	1.51	-2.24	2.25

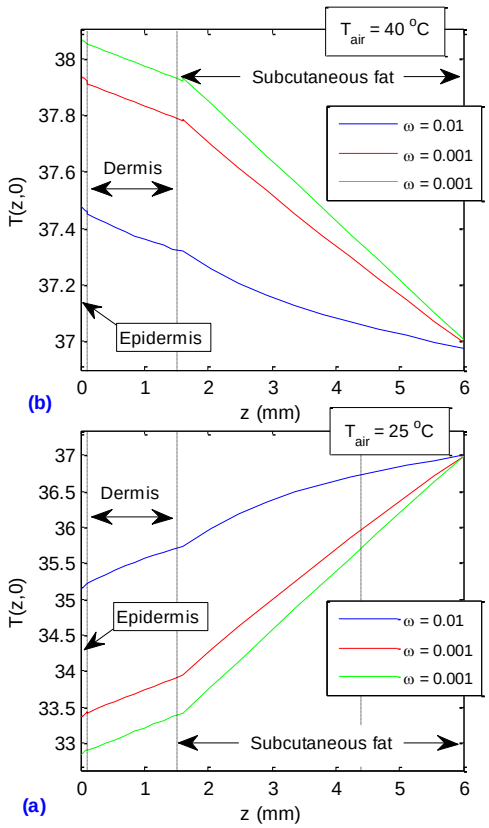

Fig. 2. Effect of blood perfusion rate and air temperature on the equilibrium temperature distribution of the skin layers: a) T_{air} = 25ºC, b) T_{air} = 40ºC

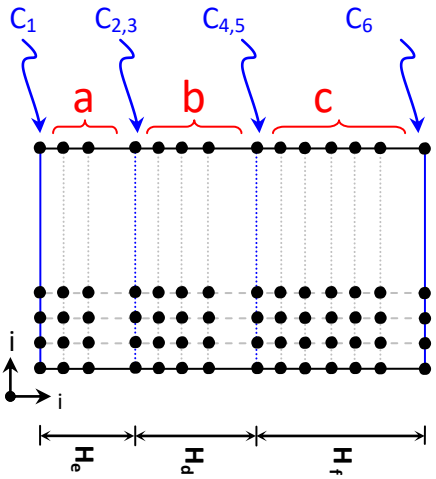

Fig. 3. Finite-difference mesh used for three skin layers

Temperature distribution resulted from an external heat source

Temperature distribution in the three skin layers generally consists of the equilibrium temperature distribution and the temperature distribution resulted from an external heat source. Therefore, this distribution can be calculated by solving the bio-heat transfer equations (4) under the boundary conditions provided in equations (5). Nevertheless, although the general solution of these partial differential equations is available, the particular solution of these equations by using the boundary conditions provided in equations (5) is inaccessible with the current science. We accordingly solved these partial differential equations by using the backward finite-difference method (BFDM) [41, 42], which is usually known as the backward Euler method. The following equations present the approximate differential equations obtained from equations (4) and (5) by using the BFDM:

$$
\begin{cases}
a: \left[\frac{\rho_e c_e}{\Delta t}+\frac{2k_e}{\Delta z_e^2}\right]T_{ei,j}-\frac{\rho_e c_e}{\Delta t}T_{ei,j-1}-\frac{k_e}{\Delta z_e^2}\left[T_{ei+1,j}+T_{ei-1,j}\right]=Q_{e,met} \\
b: \left[\frac{\rho_d c_d}{\Delta t}+\frac{2k_d}{\Delta z_d^2}-\omega_b\rho_b c_b(1-\mu)\right]T_{di,j}-\frac{\rho_d c_d}{\Delta t}T_{di,j-1}-\frac{k_d}{\Delta z_d^2}\left[T_{di+1,j}+T_{di-1,j}\right] \\
\qquad =Q_{d,met}-\omega_b\rho_b c_b(1-\mu)T_a \\
c: \left[\frac{\rho_f c_f}{\Delta t}+\frac{2k_f}{\Delta z_f^2}-\omega_b\rho_b c_b(1-\mu)\right]T_{fi,j}-\frac{\rho_f c_f}{\Delta t}T_{fi,j-1}-\frac{k_f}{\Delta z_f^2}\left[T_{fi+1,j}+T_{fi-1,j}\right] \\
\qquad =Q_{d,met}-\omega_b\rho_b c_b(1-\mu)T_a \\
\text{----------} \\
C_1: \; T_{e1,j}=Q_{extj} \\
C_{2,3}: \; T_{d1,j}=T_{eend-1,j} \\
C_{4,5}: \; T_{f1,j}=T_{dend-1,j} \\
C_6: \; T_{fend,j}=T_C
\end{cases}
\qquad (10)
$$

where i and j are the unit vectors of the z-axis and the t-axis in finite-difference mesh, respectively. Fig. 3 provides the finite-difference mesh employed in this study. As shown in the figure, we used the approximate bio-heat transfer equations (a-c) for points located into the skin layers, and the approximate equations of boundary conditions for points located on boundaries. In other words, we computed an equation for each of the points located on the finite-difference mesh by using equations (10). Finally, we solved the system of linear equations generated by these equations by using the Gauss-Jordan elimination method, and got the temperature of each of the mesh points.

Fig. 4 indicates the effect of two different blood perfusion rates on the temperature distribution resulted from a thermal pulse of 0.25 s (Q(t)) applied on the skin surface. As seen in this figure, comparing the patterns together generally shows that increasing the blood perfusion rate in the internal layers amplifies the amount of heat absorption, because the temperature of the thermal pulse is higher than that of arterial blood (Fig. 2). Lower temperature distribution in inner layers, especially the subcutaneous fat layers, confirms this issue. These distributions also show that two internal layers, especially the subcutaneous fat layers, like a thermal inductor always disagree with any change in the thermal flow. Areas marked with the red and yellow

arrows in these patterns confirm this issue that the internal layers recoil the heat at the beginning of the thermal pulse and absorb the heat after removing the thermal pulse. In other words, since thermal flow is increased and decreased in the rising and falling edges of the thermal pulse, the internal layers, especially the subcutaneous fat layers, as a thermal inductor disagree with it in these times. Therefore, this means that the thermal response in the skin tissue against an external heat source can become from a conductor an insulator and conversely, due to changing the heat flow. This property of internal layers, in addition to reducing the amount of stress entered on internal tissues, also leads to the gradual expansion and contraction of skin tissue, which are effective processes for reducing thermal damage, especially at low temperatures. In other words, the gradual expansion and contraction slowly convert thermal energy into kinetic energy, which result in less thermal damage. In the next section, we calculated the thermal expansion of the skin.

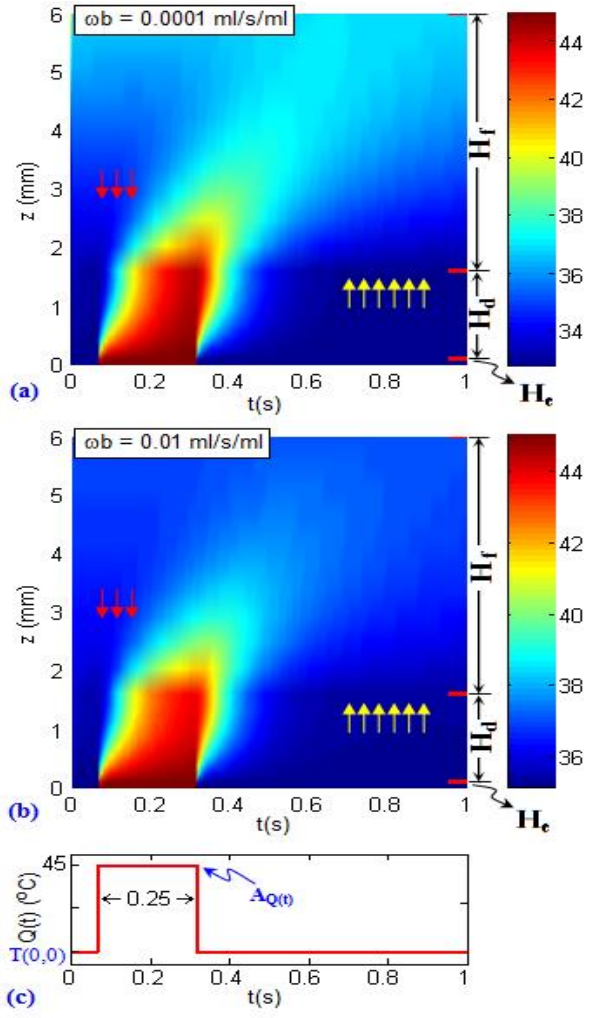

Fig. 4. Effect of two different blood perfusion rates on temperature distribution resulted from a thermal pulse: a) 0.0001 ml/s/ml, b) 0.01 ml/s/ml, c) the thermal pulse.

Thermal expansion in three skin layers

Strain according to Hooke's Law in 1D is defined as follows [43]:

$$\varepsilon = \varepsilon_M + \varepsilon_T \tag{11}$$

where ε_M and ε_T are strains resulted from the mechanical and thermal loading. Since we have only a thermal loading on the skin tissue (ΔT), the term relevant to mechanical strain was zero. Therefore, the strain is:

$$\varepsilon(t) = \varepsilon_T(t) = \alpha_s \Delta T(t) = \frac{\Delta\delta(t)}{\Delta x} \tag{12}$$

where α_s is the linear coefficient of thermal expansion and δ is thermal expansion. According to this equation, we can calculate total thermal expansion as follows:

$$\delta(t) \approx \sum_i \alpha_s \Delta T_i(t) \Delta x_i(t) \tag{13}$$

Fig. 5 provides a part of finite-difference mesh in Fig. 3 that visually describes equation (13). Since we considered the temperature of internal tissue equal to the core temperature (T_c) and also, since α_{air} is much larger than α_s, equation (13) is an acceptable estimation for thermal expansion created in the skin.

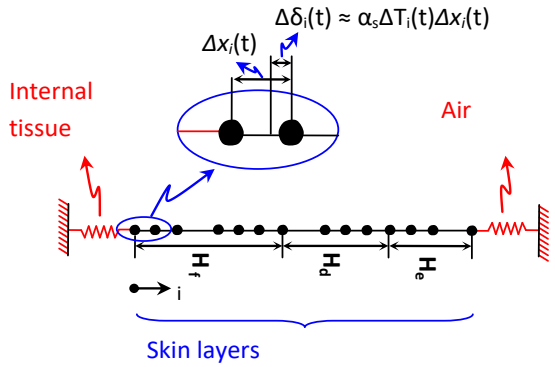

Fig. 5. A part of finite-difference mesh in Fig. 3 employed for calculating the thermal expansion of skin layers.

Fig. 6 illustrates the thermal expansion resulted from the temperature distribution in Fig. 4a. As shown in this figure, total thermal expansion has a gradual increase during applying the thermal pulse, and a gradual decrease after removing the thermal pulse, so that the time constant of the contraction phase is larger than that of the expansion phase in the skin layers. Comparing the thermal expansion of the two internal layers with total thermal expansion generally shows that the cause of a larger time constant in the contraction phase is the subcutaneous fat layer. The cause of the smaller time constant in the expansion phase is the dermis layer.

Besides, although the amount of total thermal expansion is negligible at low temperatures and the

kinetic energy generated by these temperatures cannot disrupt the molecular bonds of proteins, the amount of total thermal expansion at high temperatures due to the excessive kinetic energy can disrupt the molecular bonds of proteins. Fig. 7 shows the total thermal expansion resulted from the thermal pulses of 0.25 s with different amplitudes ($A_{Q(t)}$). As seen in this figure, increasing the temperatures exponentially increases the amount of thermal expansion. Therefore, this amount of thermal expansion coupled with its equivalent kinetic energy at high temperatures can simply disrupt the molecular bonds of protein. This discontinuity changes the nature of materials, and its result is thermal damage. In the following section, we investigated the thermal damage generated by a temperature distribution in the skin.

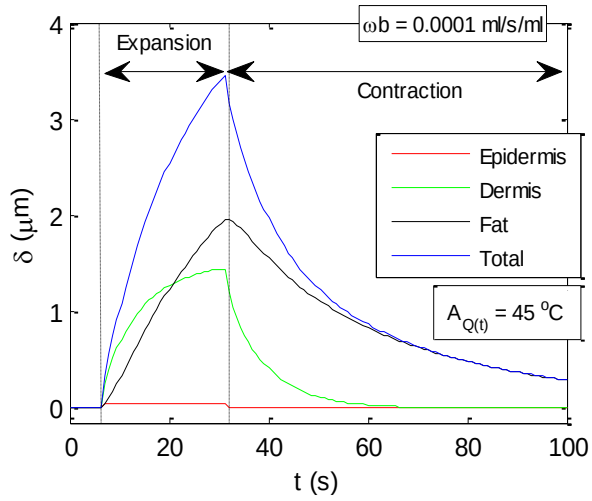

Fig. 6. Thermal expansion in the skin layers

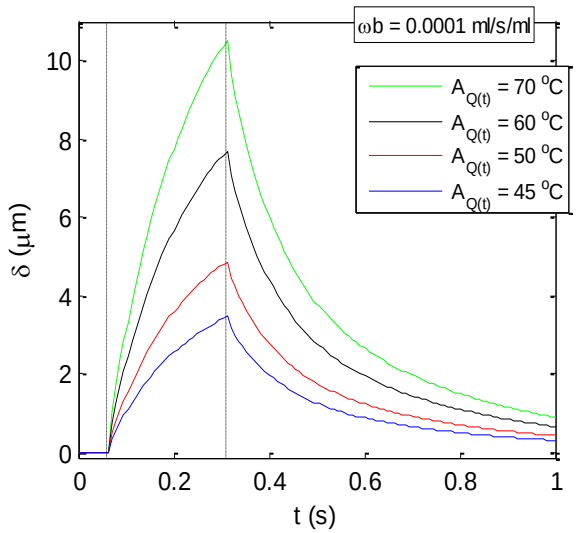

Fig. 7. Thermal damage resulting from thermal pulses of 0.25 s with different amplitudes (see $A_{Q(t)}$ in Fig. 4) in three skin layers.

Total thermal expansion resulted from the thermal pulses of 0.25 s with different amplitudes (α_s = 0.0001).

Thermal damage in three skin layers

It is obvious that the temperature is a very important factor to enhance the rate of successful collisions between the particles of a reactant. Therefore, increasing the temperature in the skin tissue amplifies the kinetic energy and causes that the molecules vibrate rapidly and violently. This vibration in the molecules also increases the rate of protein denaturation, which outcome at long term is the thermal damage. So, the thermal damage (Ω) in the skin tissue generally depends on the rate of protein denaturation (k) and exposure time (t) at a given temperature. Henriques and Moritz [44, 45] have accordingly proposed that the thermal damage in a tissue can be measured by the Arrhenius equation [46] as follows:

$$k(T(z)) = \frac{d\Omega(z)}{dt} = Ae^{-\frac{E_a}{R[T(z)+273.15]}} \quad (14)$$

or, equivalently:

$$\Omega(z) = \int_0^t Ae^{-\frac{E_a}{R[T(z)+273.15]}}dt \quad (15)$$

where R = 8.314 $J.mol^{-1}.K^{-1}$ is the universal gas constant. A is collision frequency, which has a non-linear relationship with activation energy (Ea) [47]. E_a = 21149.324 + 2688.367 ln(A).

In the present study, the burn injury in the skin is calculated by using the burn integration of 15, with the collision frequency A = 2.1×10^{98} (E_a = 75005 $J.mol^{-1}$). Note that it is now widely accepted that Ω = 0.53, first degree burn; Ω = 1, second degree burn; $\Omega = 10^4$, third degree burn [15].

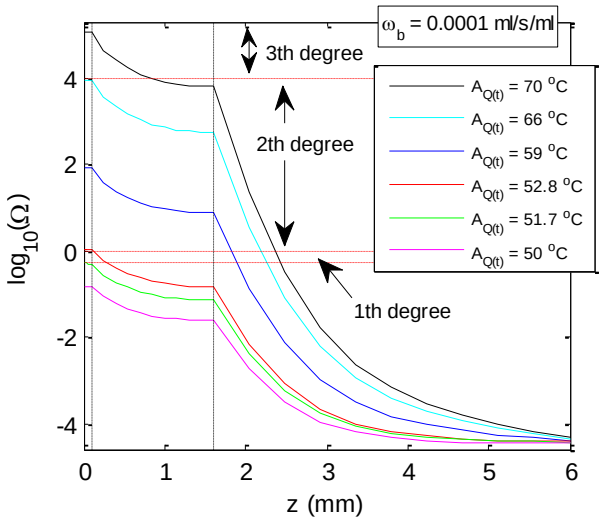

Fig. 8. Thermal damage resulting from thermal pulses of 0.25 s with different amplitudes (see $A_{Q(t)}$ in Fig 4) in three skin layers.

Fig. 8 presents the thermal damage resulted from thermal pulses of 0.25 s with different amplitudes for three skin layers. To better display the status of thermal damage in each of the skin layers, we reported its logarithmic values. The curves of Fig 8 actually indicate that a thermal pulse of 0.25 s in a narrow temperature band (51.8°C to 52.8°C) can create a first-degree burn on the two external layers of skin, especially the epidermis layers. Interestingly, the most severe type of this burn, which occurs in $\Omega \approx 1$ ($T \approx 52.8$°C), only involves a very small part of dermis layers, while the second-degree burn, which is generated by a thermal pulse of 0.25 s in a wider temperature band (52.8°C to 66.8°C), involves a significant part of dermis layers. Hence, the symptoms of this burn often are blisters and severe pain. But the most serious type of skin burn, i.e. the third-degree burn, which is generated by thermal pulses above 66°C, burns the epidermis and dermis layers and a significant part of the subcutaneous fat layer. Hence, this burn leads to the destruction of the sensory nerve endings of the outer layers. Nevertheless, although the results of Fig. 8 reported a critical condition for skin at high temperatures, the blood vessels in the two internal layers can reduce the amount of thermal damage by regulating the blood perfusion rates. Fig. 9 shows the effect of different blood perfusion rates on the thermal damage resulted from thermal pulses of 0.25 s.

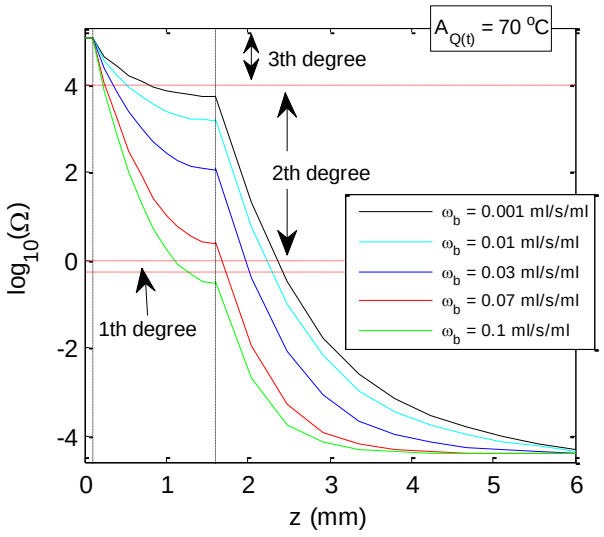

Fig. 9. Effect of different blood perfusion rates on the thermal damage led by thermal pulses of 0.25 s in the three skin layers.

As shown in this figure, increasing the blood perfusion rate significantly decreases the thermal damage in the dermis and subcutaneous fat layers. In other words, the blood vessels with more heat absorption in the higher blood perfusion rate try to hold the skin temperature at the blood temperature (37°C). This process in the vessels leads to reduction of the thermal damage at 0.25 s. In the next section, we presented a brief conclusion about the results obtained in this research.

DISCUSSION AND CONCLUSION

As stated, some of the researchers [1, 30] generally reported that increasing the blood perfusion rate only reduces the temperature of skin layers, while analytical studying the one-dimensional heat transfer model developed in this work for three-layer skin showed that the thermomechanical responses generated by the laminar structure of skin tissue coupled with the blood vessels penetrated in skin layers extremely depend on the skin surface temperature (Fig. 2). In fact, this temperature can completely reverse the effects of the blood perfusion rate, so that if the skin surface temperature is lower than the arterial blood temperature, increasing the blood perfusion rate exponentially enhances the temperature of skin layers (Fig. 2a). Conversely, if the skin surface temperature is higher than the arterial blood temperature, increasing the blood perfusion rate exponentially reduces the temperature of three skin layers (Fig. 2b). This means that the heat adsorption and desorption performed by the blood vessels depend on the temperature gradient between the arterial blood temperature and the temperature of each point from the skin tissue. Furthermore, the temperature of each point from the skin tissue is proportional to the boundary conditions, especially the skin surface temperature. Therefore, the blood perfusion rate has not the same effect on all the points of skin tissue. The temperature distributions of the three skin layers for two different blood perfusion rates in Fig 4 confirm this issue. These temperature distributions also confirm that thermal and structural properties (Table 1) due to their special arrangement in different skin layers give special flexibility to the skin against heat. For example, as shown in Table 1, the thermal conductivity of the subcutaneous fat layer (0.185 W/m°C) is less than that of the dermis layer (0.445 W/m°C). This difference in the thermal conductivity of the two layers leads to gradual spreading of the heat in the subcutaneous fat layer and quick spreading of the heat in the dermis layer. This heat transfer process has a direct effect on the amount of heat absorbed by the blood vessels. In other words, the subcutaneous fat layer, due to its greater thickness (4.4 mm) absorbs more heat than the dermis layer. Therefore, the dermis layer experiences a higher temperature than the subcutaneous fat layer (Fig. 4). This means that the dermis layer converts more thermal energy into kinetic energy. Consequently, the thermal expansion of the dermis layer exceeds that of the subcutaneous fat layer (Fig. 6). This thermal expansion along with

its equivalent kinetic energy at low temperatures can be eliminated by the blood vessels, but the kinetic energy generated by the high temperatures cannot be eliminated by the blood vessels. Hence, the unabsorbed kinetic energy exponentially increases the distance (and motion) between constituents of matter, whose outcome is a thermal expansion (Fig. 7). This critical status disrupts bonds between the constituents of materials and changes the nature of materials. The result of this change in the tissue is thermal damage, which usually appears as an injury (Fig. 8).

Interestingly, the epidermis layer, despite having a lower thermal conductivity (0.235 W/m^{o}C) than the dermis layer, tolerates high temperature due to the low thickness and proximity to the skin surface (Fig. 4). This high temperature in the epidermis layer creates thermal expansion, which is relatively less than that of other layers. Nevertheless, this expansion compared with the thickness of the epidermis layer (0.1 mm) is remarkable, so that usually creates the most damage in the burning conditions, i.e. high temperature and exposure time at this temperature. Fig. 8 well confirms this issue. This figure also confirms that the burn degree in all of the skin layers is directly proportional to the temperature applied to the skin surface and can be reduced by increasing the blood perfusion rate (Fig. 9). Some of the researchers [1, 14, 15] nonetheless reported that the blood perfusion rate has little influence on burn damage; while they considered that this rate has a high influence on the temperature distribution in the skin. It is remarkable that these researchers used equation (13) for calculating the burn damage, in which there is a direct proportion between the temperature and the thermal damage. Therefore, this direct proportion does not confirm the outcome reported by these researchers.

There are also limitations in our paper. First, we have assumed constant properties for each of the skin layers, while these properties are usually non-constant, especially at the boundary of layers. Second, we have considered the present model as one-dimensional one, but the skin is a spatial object. Third, our model includes three layers. Accordingly, we assumed the boundary condition between the subcutaneous fat layer and the fat layer equal to the core temperature, while the internal layers (fat, muscle and bone) have a non-stationary temperature distribution.

Nevertheless, although the elimination of each of the limitations will be an interesting start point for future works, the results reported in the previous section show that the present model has an adequate ability to model the heat transfer and to evaluate the burn injuries in multi-layer skin. Therefore, this model can be very interesting for improving medical applications such as the local hyperthermia techniques and for evaluating the burn injuries. The outcomes obtained from this model can be also validated and employed in laminar insulations used in building facilities, in which heating installations usually penetrate in some layers.

REFERENCES

1. F. Xu, T.J. Lu, K. A. Seffen, *Journal of the Mechanics and Physics of Solids*, **56**(5), 1852 (2008).
2. D. A. Stewart, T. R. Gowrishankar, J. C. Weaver, *IEEE Transactions on Plasma Science*, **34**(4), 1480 (2006).
3. B. Stec, A. Dobrowolski, W. Susek, *IEEE Transactions on Biomedical Engineering*, **51**(3), 548 (2004).
4. N. S. Sadick, J. Shaoul, *Journal of Cosmetic and Laser Therapy*, **6**(1), 21 (2004).
5. R. A. Weiss, M. A. Weiss, G. Munavalli, K. L. Beasley, *Journal of Drugs in Dermatology JDD*,.**5**(8), 707 (2006).
6. Y.-K. Tay, C. Kwok, E. Tan, *Lasers in Surgery and Medicine*, **38**(3), 196 (2006).
7. D. J. Goldberg, *Expert Review of Medical Devices*, **4**(2), 253 (2007).
8. K. R. Diller, I. C. Young, Modeling of Bioheat Transfer Processes at High and Low Temperatures, in: Advances in Heat Transfer, Elsevier, 1992, p. 157.
9. J. van der Zee, *Annals of Oncology*, **13**(8), 1173 (2002).
10. P. Wust, B. Hildebrandt, G. Sreenivasa, B. Rau, J. Gellermann, H. Riess, R. Felix, P. M. Schlag, *The Lancet Oncology*, **3**(8), 487 (2002).
11. M. R. Habib, D. L. Morris, Local and Regional Hyperthermia, in: Induction Chemotherapy: Systemic and Locoregional, K. R. Aigner, F. O. Stephens (eds.) Springer International Publishing: Cham., p. 53.
12. P. Wolf, Innovations 2016 in biological cancer therapy, a guide for patients and their relatives, Naturasanitas, 2008, p. 31.
13. G. F. Baronzio, E. D. Hager, Hyperthermia in Cancer Treatment: A Primer, Springer US, 2008.
14. F. Xu, *Applied Mechanics Reviews*, **62**(5), 050801 (2009).
15. F. Xu, T. Wen, T. J. Lu, K. A. Seffen, *Journal of the Mechanical Behavior of Biomedical Materials*, **1**(2), 172 (2008).
16. E. H. Wissler, *Journal of Applied Physiology*, **85**(1), 35 (1998).
17. J. Liu, L. X. Xu, *International Journal of Heat and Mass Transfer*, **43**(16), 2827 (2000).
18. T. A. Balasubramaniam, H. F. Bowman, *Journal of Heat Transfer*, **96**(3), 296 (1974).
19. M. M. Chen, K. R. Holmes, V. Rupinskas, *Journal of Biomechanical Engineering*, **103**(4), 253 (1981).
20. R. C. Eberhart, A. Shitzer, E. J. Hernandez, *Annals of the New York Academy of Sciences*, **335**, 107 (1980).
21. D. A. Torvi, J. D. Dale, *Journal of Biomechanical Engineering*, **116**(3), 250 (1994).

22. C. J. Andrews, L. Cuttle, M. J. Simpson, *International Journal of Heat and Mass Transfer*, **101**, 542 (2016).
23. R. Vyas, M. L. Rustgi, *Medical Physics*, **19**(5), 1319 (1992).
24. W. H. Newman, P. P. Lele, H. F. Bowman, *International Journal of Hyperthermia: The Official Journal of European Society for Hyperthermic Oncology, North American Hyperthermia Group*, **6**(4), 771 (1990).
25. L. Zhu, S. Weinbaum, *Journal of Biomechanical Engineering*, **117**(1), 64 (1995).
26. J. W. Durkee, P. P. Antich, C. E. Lee, *Physics in Medicine and Biology*, **35**(7), 847 (1990).
27. J. W. Durkee, P. P. Antich, C. E. Lee, *Physics in Medicine and Biology*, **35**(7), 869 (1990).
28. J. J. W. Lagendijk, *Physics in Medicine and Biology*, **45**(5), R61 (2000).
29. E. Kengne, I. Mellal, A. Lakhssassi, Bioheat transfer problems with spatial or transient heating on skin surface or inside biological bodies, in: 7th International Conference on Biomedical Engineering and Informatics, 2014.
30. Z.-S. Deng, J. Liu, *Journal of Biomechanical Engineering*, **124**(6), 638 (2002).
31. S. Y. Lin, T. M. Chou, Numerical Analysis of the Pennes Bioheat Transfer Equation on Skin Surface, in: Third International Conference on Robot, Vision and Signal Processing (RVSP), 2015.
32. D. Lai, Q. Chen, *Energy and Buildings*, **118,** 114 (2016).
33. M. Strakowska, G. de Mey, B. Vitzek, M. Strzelecki, *Journal of Mechanics in Medicine and Biology*, 15(4), 1550044 (2015).
34. M. Geerligs, *Journal of Philips Research*, 1 (2006).
35. J. C. Chato, *Journal of Biomechanical Engineering*, **102**(2), 110 (1980).
36. M. M. Chen, K. R. Holmes, *Annals of the New York Academy of Sciences*, **335,** 137 (1980).
37. J. Crezee, J. J. W. Lagendijk, *Physics in Medicine and Biology*, **37**(6), 1321 (1992).
38. H. H. Pennes, *Journal of Applied Physiology*, **85**(1), 5 (1998).
39. J. S. Hutchison, *The New England Journal of Medicine*, **358**(23), 2447 (2008).
40. Xin Gui, F. H. George, Proc. International symposium on symbolic and algebraic computation. 1997, ACM, Kihei, Maui, Hawaii, USA.
41. D. G. Zill, M. R. Cullen, Advanced Engineering Mathematics, Jones and Bartlett Publishers, 2006:
42. N. O. a. S. Matthew, Numerical Techniques in Electromagnetics, CRC Press, 2001.
43. L. P. Kollar, Mechanics of Composite Structure. Cambridge University Press, Cambridge, 2003.
44. F. C. Henriques, A. R. Moritz, *The American Journal of Pathology*, **23**(4), 530 (1947).
45. A. R. Moritz, F. C. Henriques, *The American Journal of Pathology*, **23**(5), 695 (1947).
46. K. J. Laidler, Chemical Kinetics, Pearson Education, 1987.
47. N. T. Wright, *Journal of Biomechanical Engineering*, **125**(2), 300 (2003).